A Brillouin scattering study of the quasi-one-dimensional blue bronze, $K_{0.3}MoO_3$

2000 J. Phys.: Condens. Matter 12 L225

(http://iopscience.iop.org/0953-8984/12/12/103)

J. Phys.: Condens. Matter **12** (2000) L225–L231. Printed in the UK PII: S0953-8984(00)11545-0

LETTER TO THE EDITOR

A Brillouin scattering study of the quasi-one-dimensional blue bronze, $K_{0.3}MoO_3$

P Murugavel†‡, Chandrabhas Narayana†, Ajay K Sood†‡ and C N R Rao†‡

† Chemistry and Physics of Materials Unit, Jawaharlal Nehru Centre for Advanced Scientific Research, Jakkur PO, Bangalore 560 064, India

‡ Indian Institute of Science, Bangalore 560 012, India

Received 2 February 2000

Abstract. Brillouin scattering measurements have been carried out for the first time on $K_{0.3}MoO_3$. The spectrum reveals two bulk modes at 18 and 27 GHz and a Rayleigh surface mode at 6 GHz. Both the bulk modes and the surface mode exhibit changes at the Peierls transition (180 K). Interestingly, the 18 GHz mode also shows softening at the incommensurate–commensurate transition around 100 K, suggesting the important role of phasons.

Collective electron transport due to the sliding of the charge density wave (CDW) has been a topic of much interest [1]. Many of the quasi-one-dimensional solids undergo a second-order metal–insulator transition (Peierls transition) into the CDW state. Among these materials, the blue potassium molybdenum bronze, $K_{0.3}MoO_3$, is of particular interest. This bronze exhibits the Peierls transition around 180 K (T_p), as well as highly anisotropic quasi-one-dimensional properties [2]. The conductivity also shows a non-linear behaviour due to the sliding of the CDW [3,4]. $K_{0.3}MoO_3$ also undergoes an incommensurate to commensurate (IC–C) transition near 100 K as evidenced from x-ray and neutron scattering studies [5]. The Young's modulus of $K_{0.3}MoO_3$ along the [102] direction shows a large dip at T_p, whereas along the chain [010] direction (b-axis), the anomaly is much smaller [6]. The elastic constant C_{22} and the sound velocity of the longitudinal acoustic (LA) mode along the $[20\bar{1}]$ direction measured by ultrasonic absorption shows softening with increasing temperature without any anomaly [7]. However, the sound velocity of the LA mode generated along the [102] direction shows a dip at T_p. Similarly, the thermal expansion coefficient along the [102] direction shows an anomaly at T_p which is not seen along the [010] direction, nor along the $[20\bar{1}]$ direction [8]. These measurements, however, were limited to 80 K and hence did not cover the interesting consequences of the IC–C transition. We have carried out Brillouin scattering experiments on $K_{0.3}MoO_3$ for the first time, in order to investigate the nature of changes around T_p, and equally importantly, to explore whether the IC–C transition manifests itself in some way. The study has indeed revealed interesting changes of the bulk and surface modes at T_p, and anomalous softening of one of the bulk mode around the IC–C transition.

Single crystals of $K_{0.3}MoO_3$ (face-centred monoclinic structure) were freshly cleaved into thin plates of typical dimensions of $3 \times 2 \times 0.5$ mm, corresponding to the [010], [102] and $[20\bar{1}]$ directions, respectively. Based on a Weisenberg photograph, the presence of [010] and [102] directions in the cleavage plane $(20\bar{1})$ was established. Brillouin experiments were carried out in back-scattering geometry with light incident at an angle $\theta = 45^\circ$ to the $[20\bar{1}]$ axis (see the inset of figure 1). The measurements were made using an incident wavelength (λ) of 532 nm (Coherent, Inc., USA, make DPSS 532-400) at a power of $\sim$ 50 mW, with the incident

polarization ($\widehat{e_i}$) along either the [010] or [102] axis. Scattered light was analysed without polarization selection using a Sandercock-type six-pass tandem Fabry–Perot interferrometer (TFP), which has a finesse greater than 100 [9]. The TFP was placed on a dynamic vibrational isolation system to remove external influences which could distort the mirror spacing. Spectra presented in this work were recorded using a multichannel scaler with 512 channels and the typical accumulations of 3000–8000 passes were done with 0.768 s per pass. The lineshape parameters, peak freqency, full-width at half maximum (FWHM) and area were extracted by non-linear least square fitting of the data with a Lorentzian function with an appropriate baseline.

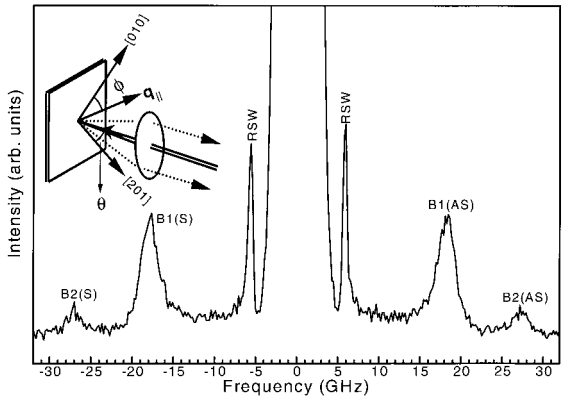

Figure 1. Brillouin spectrum of $K_{0.3}MoO_3$ at 300 K at $\phi = 30^\circ$. The inset shows the scattering geometry.

Figure 1 shows the Brillouin spectrum of $K_{0.3}MoO_3$ at 300 K with $\widehat{e_i}$ at an angle of 30° with the [010] axis. The spectrum reveals three modes around 6, 18 and 27 GHz, labelled as RSW, B1 and B2. S and AS refer to Stokes and anti-Stokes scattering. The sharpness of the RSW mode suggests it to be a Rayleigh surface wave (RSW). Figure 2(a) shows the dependence of this mode frequency (ν_R) on $q_\parallel$, the component of the wavevector parallel to the surface given by $q_\parallel = (4\pi/\lambda)\sin\theta$. The solid line in this inset is a fit to $2\pi\nu_R = v_R q_\parallel$, which gives $v_R = 1.92 \times 10^5$ cm sec^{-1}. Figure 2(b) shows the dependence of v_R on the angle ϕ between $q_\parallel$ and [010] direction. The sinusoidal variation of v_R as a function of ϕ (for a given $q_\parallel$) confirms that the 6 GHz peak in figure 1 is associated with the RSW. The other two modes B1 and B2 are bulk modes. With $\widehat{e_i} \parallel [010]$, only the B1 mode is observed, whereas the B2 mode is observed for $\widehat{e_i} \parallel [102]$. Further, these modes were seen only when $\widehat{e_i} \parallel \widehat{e_s}$, where $\widehat{e_s}$ is the polarization of the scattered light.

The temperature dependence of all three mode frequencies is shown in figure 3, where $\Delta\omega/\omega = (\omega(T) - \omega(300\text{ K}))/\omega(300\text{ K})$. The B1 mode shows usual stiffening as temperature is lowered due to reduced anharmonicity. The error bars in the frequency do not permit us to conclude any significant changes at T_p. The solid line is a fit to $\Delta\omega/\omega = A + BT$ between 300 K and 70 K, with $A = 4.96$ and $B = 0.014$ K^{-1}. However, the softening below 70 K is very anomalous. Figure 3(b) shows the temperature dependence of the B2 mode frequency ($\nu_{[102]}$) up to 100 K. We were not able to follow this weak mode below 100 K as it merged with the reflection scattering peak (an artifact) [10]. The behaviour of these bulk modes around T_p, i.e. the dip in $\nu_{[102]}$ and less anomaly in $\nu_{[010]}$, is similar to the data on Young's Modulus [6], ultrasonic measurements [7] and thermal expansion coefficient [8]. The

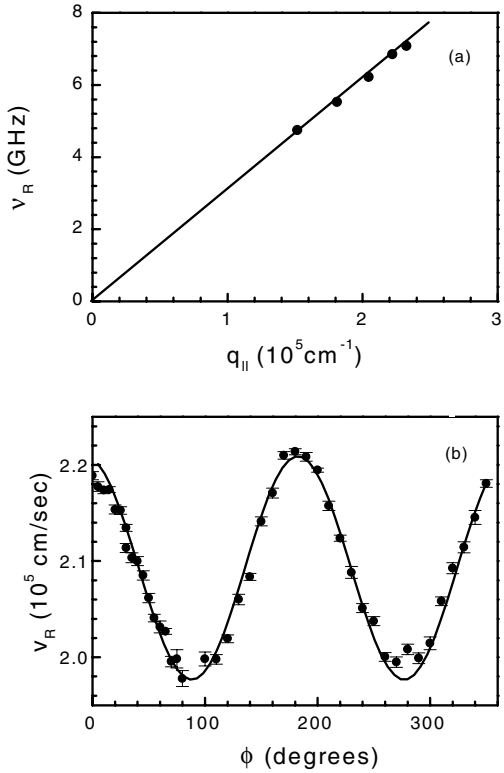

Figure 2. (a) Frequency dependence of the RSW mode (ν_R) as a function of $q_\parallel$. The solid line is a linear fit, as explained in the text. (b) The velocity dependence of RSW mode (v_R) as function of angle ϕ (between [010] and $\mathbf{q}_\parallel$ (see inset of figure 1)). A sine function is fitted to the data represented by the solid line.

anisotropy in the temperature dependence of these quantities arises due to the fact that the lattice distortion is caused by the displacement of Mo(3) ions along the [102] direction, with very little displacement along the [010] and [20$\bar{1}$] directions [11].

The RSW mode frequency also shows a change in temperature dependence at the Peierls transition (figure 3(c)). This is expected, as the surface mode is associated with the cleavage plane (20$\bar{1}$). The solid lines are fits to the linear temperature dependence with slope $B = 0.025$ K^{-1} for $T > T_p$ and $B = 0.049$ K^{-1} for $T < T_p$. Based on the lattice distortions along various directions derived from x-ray diffraction measurements [12], we would expect only small changes in the properties along the cleavage plane. We will now discuss the temperature dependence of B2 mode frequency shown in figure 3(b). For a second-order phase transition, assuming that the singular free energy depends only on stress σ, the changes in elastic constants (ΔC) can be related to the specific heat changes ΔC_p at T_p [13, 14]

$$\frac{\Delta C}{C_\circ} \sim -C_\circ \left(\frac{\partial T_p}{\partial \sigma}\right)^2 \frac{\Delta C_p}{T} \tag{1}$$

where $C_\circ$ is the elastic constant at 300 K, $\partial T_p/\partial\sigma$ is the change in transition temperature with pressure (~ -1.4 K kbar^{-1} as measured experimentally [15]). Assuming that the density and refractive index changes across the second-order transition are negligible, the change in Brillouin mode frequency $2(\Delta\omega/\omega) = \Delta C/C$. The solid line in figure 3(b) is a fit to

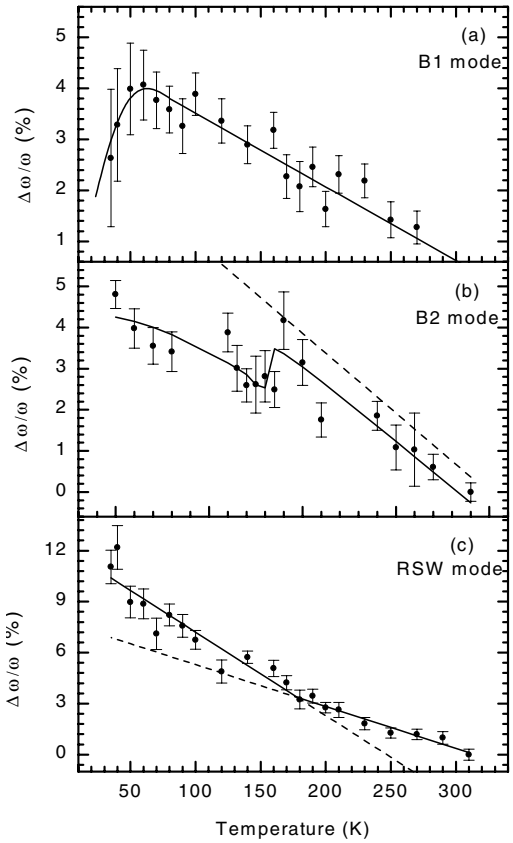

Figure 3. Relative percentage changes of the phonon frequency ($\Delta\omega/\omega$) as a function of temperature for the three modes (B1, B2 and RSW). The lines are fits to the equations, as explained in the text.

equation (1) along with the linear background shown by the dotted line. The specific heat variation was taken as follows [16]:

$$\Delta C_p = A_1^+ t^{-\alpha}[1 + A_2^+ t^{\Delta}] + A_3^+ t^{-\gamma}[1 + A_4^+ t^{\Delta}] \qquad (T \geqslant T_p) \tag{2}$$

$$\Delta C_p = A_1^- |t|^{-\alpha}[1 + A_2^- |t|^{\Delta}] + A_3^- |t|^{-\gamma}[1 + A_4^- |t|^{\Delta}] \qquad (T \leqslant T_p) \tag{3}$$

where $t = (T - T_p)$ and the universal constants $\alpha = 0.11$, $\Delta = 0.51$ and $\gamma = 1.33$. The coefficients are taken to obey $A_1^+/A_1^- = 0.5$ and $A_3^+/A_3^- = 4.92$. It can be seen that the dip in $\Delta\omega/\omega$ essentially reflects the peak in the specific heat at T_p

The softening of B1 mode below 100 K in figure 3(a) is due to an IC–C transition as explained below. Below T_p, there are modes corresponding to the collective excitation of the amplitude (called amplitudon) and phase (called phason) of the CDW modulation [17]. The intrachain deformations of the CDW result in charge distribution leading to long range Coulomb forces. As the temperature is lowered from T_p, these Coulomb forces are screened by the quasi-particles thermally excited through the Peierls gap. This results in acoustic-like phason dispersion in the chain direction. The phason velocity along chain direction at 100 K is $\sim 8 \times 10^5$ cm s^{-1} [18]. At low temperatures screening is considerably reduced, thereby increasing the rigidity of the CDW. Hence the longitudinal phason becomes optic-like for the

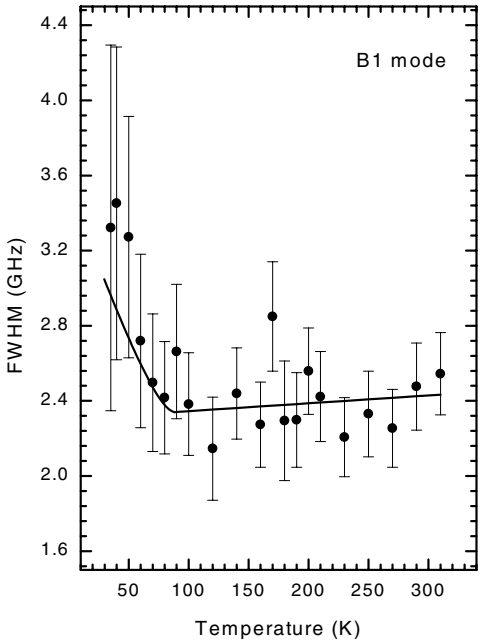

Figure 4. The FWHM of B1 mode as a function of temperature. The solid line upto 70 K is a linear fit to the data, below which the line is drawn as a guide to the eye.

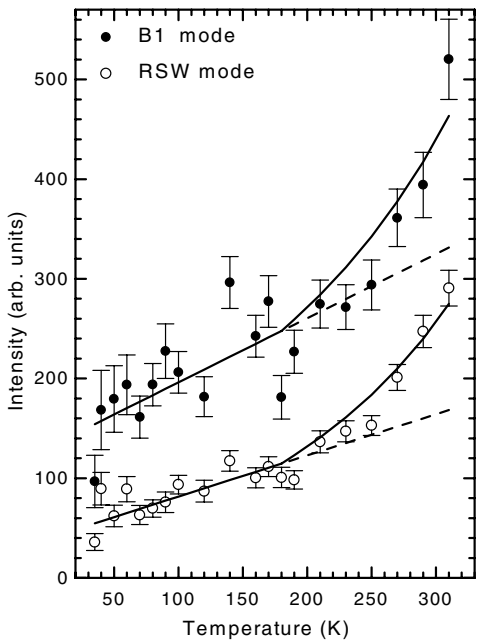

Figure 5. Intensity of B1 and RSW modes as a function of temperature. The solid lines are fits as explained in the text. The dashed line is the extrapolation of the low temperature fit.

incommensurate phase. However, if the low temperature phase is commensurate, the phason will tend to be acoustic-like due to sliding of rigid CDW. The damping of these phasons is also reduced at low temperatures. This will result in increased phonon–phason interactions in the commensurate phase. The enhanced self-energy (Σ) contributes to the phonon, resulting in phonon softening (due to the real part of Σ) and phonon damping (due to the imaginary part of Σ). We would therefore expect a change in the FWHM around the IC–C transition. The temperature dependence of the FWHM for the B1 mode does indeed exhibit a clear change, as shown in figure 4.

Temperature dependence of the intensity of the B1 and RSW modes is shown in figure 5. In the low temperature phase, intensity increase linearly with temperature (shown by the fitted solid line $I = C + DT$) as expected from the Bose–Einstein factor. The extra contribution to the intensity above T_p in the metallic phase comes from the decrease in conductivity, as this would increase the penetration depth δ of the light ($\delta \propto 1/\sqrt{\sigma}$). Taking the measured values of conductivity along the b-direction from [4], the solid line above T_p is a fit to $C + DT + E(1/\sqrt{\sigma(T)} - 1/\sqrt{\sigma(T_p)})$.

In conclusion, Brillouin scattering experiments reveal distinct signatures of the Peierls transition (180 K) as well as of the incommesurate–commensurate transition ($\sim$ 100 K) in the blue bronze. The difference in temperature dependence of the bulk modes at 18 GHz and 27 GHz at the Peierls transition can be related to differences in lattice distortions along different axes; lattice distortion is greater along [102] as compared to [010] and [20$\bar{1}$]. The dip in the frequency of the B2 mode at T_p is related to the enhancement of specific heat C_p due to critical fluctuations. The softening of the B1 mode at the IC–C transition and the temperature variation in the FWHM of this mode clearly demonstrates the interesting role of phasons in providing decay channels for the acoustic modes. It will be interesting to see the effect of depinning of the CDW on phonon lineshape parameters in the non-linear conduction regime.

We wish to acknowledge the help of Mr N Manoj and Professor Vijayan for the Weissenberg photographs of the crystal.

References

[1] Monceau P 1985 *Electronic Properties of Inorganic Quasi-One-Dimensional Compounds* ed P Monceau (Dordrecht: Reidel) **2** p 139
Grüner G 1988 *Rev. Mod. Phys.* **60** 1129
Thorne R E 1996 *Physics Today* **49** 42
[2] Hutiray G and Solyom J 1985 *Charge Density Waves in Solids: Springer Lecture Notes in Physics* (Berlin: Springer) **217** pp 17–22, 439–48
[3] Dumas J, Schlenker C, Marcus J and Buder R 1983 *Phys. Rev. Lett.* **50** 757
[4] Fogle W and Perletein J H 1972 *Phys. Rev.* B **6** 1402
[5] Fleming R M and Schneemeyer L F 1985 *Phys. Rev.* B **31** 899
[6] Bourne L L and Zettl A 1986 *Solid State Commun.* **60** 789
Brill J W 1982 *Solid State Commun.* **41** 925
[7] Saint-Paul M and Tessema G X 1989 *Phys. Rev.* B **39** 8736
[8] Hauser M R, Plapp B B and Mozurkewich G 1991 *Phys. Rev.* B **43** 8105
[9] Lindsay S M, Anderson M W and Sandercock J R 1981 *Rev. Sci. Instrum.* **52** 1478
Nizzoli F and Sandercock J R 1990 *Dynamic Properties of Solids* ed G K Horton and A A Maradudin (Amsterdam: Elsevier) pp 281–335
[10] See figure 1 and figure 2 (135° scattering) of
Zha C-S, Hemley R J, Mao H-K, Duffy T S and Meade C 1994 *Phys. Rev.* B **50** 13105
[11] Saito M, Fujishita H, Saito S and Hoshino S 1985 *J. Phys. C: Solid State Phys.* **18** 2603
[12] Ghedira M, Chenavas J, Marezio M and Marcus J 1985 *J. Solid State Chem.* **57** 300
[13] Chung M, Keio Y-K, Zhan X, Figueroa E, Brill J W and Mozurkewich G 1995 *Synthetic Mater.* **71** 1891

[14] Brill J W, Chung M, Kuo Y K, Zhan X, Figueroa E and Mozurkewich A 1995 *Phys. Rev. Lett.* **74** 1182
[15] Mihaly G and Canfiel 1990 *Phys. Rev. Lett.* **64** 45
[16] Chen Z Y, Albright P C and Sengers J V 1990 *Phys. Rev.* A **41** 3161
[17] Pouget J P, Hennion B, Filippini C E and Sato M 1992 *Phys. Rev.* B **43** 8421
[18] Nakane Y and Takada S 1985 *J. Phys. Soc. Japan* **54** 977
Wong K Y M and Takada S 1987 *Phys. Rev.* B **36** 5476
[19] Travaglini G, Morke I and Wachter P 1983 *Solid State Commun.* **45** 289